# Modified Phasing Element for Broadband Reflectarray Antennas

**Wael S. Elshennawy[1, *] and Ahmed M. Attiya[2]**

**Abstract**—New phasing element for a wideband microstrip reflectarray is presented. It is formed by a phase-delay line attached to a circular ring loaded with a circular disc microstrip. The structure is enclosed by a circular ring element with a pair of gaps. It is shown that the new phasing element offers a wider bandwidth with an increased phasing range that is useful in reflectarrays phase compensation procedure. Full wave EM simulations are carried out. Good agreement exists between simulation results and measurements by using waveguide simulator method. The mutual coupling effect for a realistic reflectarray configuration with non-identical cells is accounted for by using the perturbation technique.

## 1. INTRODUCTION

Reflectarrays require at least 360° phasing range for the reflection of their elements at a given frequency of operation. This requirement is usually not obtained by typical microstrip phasing elements such as square patches on a grounded dielectric substrate. In this case, an insufficient phasing range (around 300°) and a sharp phasing slope of variable size microstrip patches lead to narrow operational bandwidth of the reflectarray. The bandwidth limitation caused by the narrow band performance of the microstrip cell element is more significant for reflectarrays. Elements with linear phase response can be used to improve the antenna bandwidth. Linearization of phase response can be done in several ways including a thick substrate, multiple stacked patches, and phase-delay lines [1–3]. Among these methods, elements with attached phase-delay lines are a good choice because of their low manufacturing cost relative to the other methods. These elements also have enough phase range, but achieving this phase-range requires relatively large space, which results in specular reflections and hence low efficiency [4].

For a single-layer reflectarray employing circular patch of variable size, the phase characteristics gradient (slope) is always smaller as in [5, 6]; however, the phase range is reduced. To overcome this shortfall, multilayers of double concentric annular-rings are suggested in [7], but the linear response over a phase range > 360° is not achievable in this case. For optimum performance, the separation between concentric annular-rings must be reduced which is not applicable in practical design. However, the inconvenience of this approach is that each layer of the multilayer reflectarray has to be manufactured separately. The assembly process should consider alignment and eliminating air gaps between different layers. As a result, the manufacturing process becomes elaborate and expensive. In [8] Guo et al. suggested to deploy double concentric ring elements with various grid spacings to achieve compromise linearity and phase range for different sub-wavelength grids $(\frac{\lambda}{2}, \frac{\lambda}{3}, \frac{\lambda}{4}, \frac{\lambda}{55})$ respectively at the expense of poorer columniation of energy in the reflectarray main beam and an increase of grating lobes levels.

Various schemes of scaling the inner radius as a function of outer radius are adopted for a single-layer in [9], and the steep slope of reflection phase curve is reduced at the expense of reduction of the phase range compared with required 360°. To overcome this problem, a single-layer double-concentric circular rings structure offering multi-resonance operation with an increased phasing range (of more

than $360°$) and low phasing slopes is investigated as viable alternatives to multilayer counterparts [10]. However, the use of double-ring phasing elements faces some manufacturing problems because of a narrow gap between rings. As a result, manufacturing errors can result in phase errors leading to a deficient reflectarray. A single-layer circular patch connected to a variable-length phase-delay line can obtain large phase range at the cost of nonlinear behavior of the phase response curve as discussed in [11–13]. Table 1 addresses the advantage and limitation of the proposed phasing element compared to other kinds of fabricated unit cells.

**Table 1.** Comparison of performance metrics on different unit cells.

| Performance Parameters | Ref. [11] | Ref. [12] | Ref. [15] | Proposed unit cell |
|---|---|---|---|---|
| Range of reflection (degree) | $> 500$ | $> 500$ | 410 | 440 |
| Operating Frequency Range (GHz) | 10.8–12.8 | 10.7–12.7 | 11–12 | 11–12 |
| Actual area $mm^2$ | $8.63 \times 8.63$ | $8.68 \times 8.68$ | $15 \times 15$ | $15 \times 15$ |
| Center Frequency (GHz) | 11.8 | 11.7 | 11.5 | 11.5 |
| Phase error relative to linear regression (Linearity) | High | High | $15°$ | $< 30°$ |
| Maximum phase difference to normal incidence | $80°$ | High | $30°$ | $55°$ |
| Robustness to manufacturing errors | Very thin phase-delay line or circular rings | | | Yes |
| Mutual coupling effect | Not available | | | Minimum |

This paper overcomes these problems by proposing a new phasing element based on single-layer microstrip elements. This phasing element is formed by a phase-delay line which is attached to a circular ring loaded with a circular disc microstrip patch and enclosed by an outside circular ring structure as shown in Fig. 1. The phase is controlled by the length of phase-delay line. The widths of the phasing element phase-delay line and circular ring are relatively thicker than those discussed in [11, 12, 14, 15], which makes the fabricated phasing elements more robust with respect to manufacturing errors. Parameters of the new phasing structure are carefully chosen in order to introduce both the required phasing range and slow phasing slope. The phase response characteristics are produced by performing full wave electromagnetic simulation of a unit cell using Ansoft HFSS. Then, the mutual coupling between nearby elements is investigated by a perturbation technique [16]. The field perturbation technique is applied to isolated, identical, and non-identical phasing elements by using REMCOM XFdtd software.
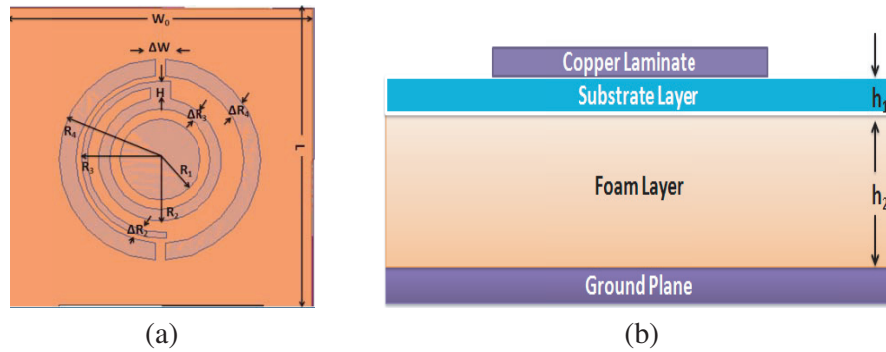


(a)                                                        (b)

**Figure 1.** Configuration of the unit cell for the proposed phasing element. (a) Top View. (b) Side View.

## 2. PHASING ELEMENT CONFIGURATION AND DESIGN PROCEDURE

The proposed phasing element is designed to operate at a center frequency of 11.5 GHz and bandwidth 1 GHz. The proposed phasing element is shown in Fig. 1. It consists of a circular ring of radius $R_2$ loaded by a circular disc microstrip patch of radius $R_1$. A phase-delay line of radius $R_3$ and width $\Delta R_3$ is attached to the circular ring through a notch of height $H$. The electrical length of the phase-delay line is $\Phi_s$. Finally, an outer circular ring of radius $R_4$ and width $\Delta R_4$ with a pair of gaps of width $\Delta W$ is surrounding the inner ring. The element is supported by a thin substrate of Rogers RT/Duroid 5880 with thickness $h_1 = 0.508$ mm and relative permittivity $\varepsilon_{r1} = 2.2$. A grounded thick foam layer of thickness $h_2 = 3.175$ mm and relative permittivity $\varepsilon_{r2} = 1.06$ is used to support this substrate. This low dielectric constant layer is used to reduce the slope of the reflection phase characteristic so that the operational bandwidth is increased. The dimension of the unit cell is chosen to be $W_0 = L = 15$ mm, which is equivalent to $0.58\lambda_0$ at the center frequency.

The design steps for the phasing element are as follows.

1) The equivalent relative permittivity and total thickness of the two substrates are given by [17].

$$\varepsilon_{rt} = \left(\sum_{n=1}^{N} \frac{h_n}{\epsilon_{rn}}\right)^{-1} \cdot \left(\sum_{n=1}^{N} h_n\right) \tag{1a}$$

$$h_t = \sum_{n=1}^{N} h_n \tag{1b}$$

2) The radius of a circular disc microstrip patch at the center frequency ($f_c$) is obtained by [11]

$$R_2 = \frac{F}{\left(1 + \frac{2h_t}{\pi \varepsilon_{rt} F} \left(Ln\left(\frac{\pi F}{2h_t}\right) + 1.7726\right)\right)^{1/2}} \tag{2}$$

$$F = \frac{8.791 \times 10^9}{f_c \sqrt{\varepsilon_{rt}}} \tag{3}$$

3) A phase-delay line with a notch is attached to a circular disc microstrip patch. By changing the dimensions of $R_1$, $\Delta R_2$, $\Delta R_3$ and $H$, a proper matching is obtained for different $\Phi_s$ at the central frequency 11.5 GHz. It should be noted that if there is a mismatch between the circular disc microstrip patch and the phase-delay line, then the relationship between phase response and $\Phi_s$ is no longer linear.

4) The final dimension of the phasing element is obtained by optimizing the phasing element geometrical parameters by using CST Microwave studio software.

Table 2 gives the final optimized parameters that attain the linear reflection phase curve for the unit cell at the operating bandwidth.

**Table 2.** Optimized parameters of phasing element.

| n | 1 | 2 | 3 | 4 |
|---|---|---|---|---|
| $R_n$ | 2.0 | 3.06 | 3.33 | 4.99 |
| $\Delta R_n$ | 2.0 | 2.5 | 3.06 | 0.83 |

The existence of an outer circular ring with a pair of gaps can serve for various applications such as circular polarization broadband reflectarrays, isolation between neighborhood unit cells thus reducing the effect of mutual coupling, supporting lower bandwidth operation by rotating it and providing broadband response. In this article, this circular ring with a pair of gaps element is used to provide an isolation between neighboring unit cells thus minimizes the impact of mutual coupling. To obtain a reflection phase response as a function of $\Phi_s$, an infinite array model is simulated by using Ansoft HFSS software with master-slave boundary and Floquet port excitation. Then, the mutual coupling between neighboring unit cells is investigated with REMCOM XFdtd software.

For the three simulation examples, isolated, identical, and non-identical, only one unit cell is illuminated by a normally incident Gaussian beam of sinusoid waveform, and the scattered field $\vec{E}^S$ and total field $\vec{E}^{tot}$ are stored within a solid box sensor enclosing the two unit cells (collection volume) assuming that the neighboring unit cell is located at a distance $d = (\infty, 15, 15)$ mm, respectively.

The perturbation factors $(\vec{\varepsilon}_{identical}(d), \vec{\varepsilon}_{non\,identical}(d))$ are calculated for the identical and non-identical unit cells as in [16]

$$PF_1 = \vec{\varepsilon}_{identical}(d) = \vec{E}^{tot}(d) - \vec{E}^{tot}(\infty) \tag{4a}$$

$$PF_2 = \vec{\varepsilon}_{non\,identical}(d) = \vec{E}^{tot}(d) - \vec{E}^{tot}(\infty) \tag{4b}$$

where $PF_1$ and $PF_2$ are the perturbation factors for identical and non-identical unit cells, and $\vec{E}^{tot}(d)$ and $\vec{E}^{tot}(\infty)$ denote the total fields for the surrounded and isolated cases, respectively. The field perturbation factor is directly related to the mutual coupling since it measures the variation induced by the reradiated field from the neighboring unit cell. Equation (8b) in [16] relates the perturbation factor to the mutual coupling where it includes the modification of parameters $S_{11}$ of illuminating unit cell and $S_{21}$ of surrounded unit cell in a way to quantify the coupling effect in terms of field strength. The perturbation technique provides an equivalent way of calculating the mutual coupling of classical array configurations.

Figure 2 represents the comparison between $PF_1$ and $PF_2$ as a function of $d$ at 11.5 GHz. It confirms that the effect of mutual coupling between neighboring unit cells is negligible for the proposed phasing element.

Figure 3 shows the phase response of the reflected wave for normal incidence with respect to $\Phi_s$ for different frequencies in the range 11.0 ~ 12.0 GHz. The results indicate a linear phase response in the range 11.0 ~ 12.0 GHz. It can be noted that by changing $\Phi_s$ up to 180°, the phase range at each of the chosen frequencies exceeds 425°, and at higher frequency the gradient is less than steep.

Figure 4 shows the phase of the reflected wave with respect to $\Phi_s$ for different angles of incidence ($\theta$ and $\phi$). It shows that linear phase response and range of phase variation is almost constant for the incident angle up to 40°. The results show that the phase performances for oblique incidence in different principal planes ($\phi = 0°, 30°, 40°$) are close. These characteristics make the proposed element a suitable choice for large-size reflectarrays. These phasing characteristics are the basis for obtaining an increased operational bandwidth of reflectarrays. Linear phase response and range of phase variation is almost constant for the incident angle up to 40° (the maximum phase difference with respect to normal incidence is 55° at $\Phi_s = 20°$ for $\phi = 40°$ and $\theta = 15°$.
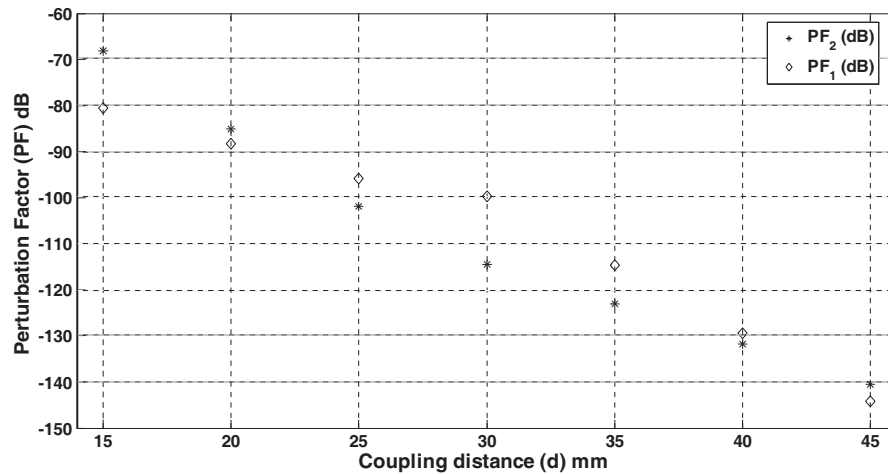


**Figure 2.** Non identical and identical perturbation factors as a function of $d$.

## 3. MEASUREMENT SETUP

For a validation of the simulation results for the reflected phase response curve, a C-band tapered waveguide section 4550-31BM1 with a dimension given in Table 3 is connected at one end with two identical unit cells as shown in Fig. 5, and the other end is connected to vector network analyzer model number 8719ES using an coaxial to waveguide adapter as shown in Fig. 6.

**Table 3.** Dimension of tapered waveguide section.

| Model Number | WG name | A (mm) | B (mm) |
|:---:|:---:|:---:|:---:|
| 4550 | WR-137 | 34.84 | 15.79 |
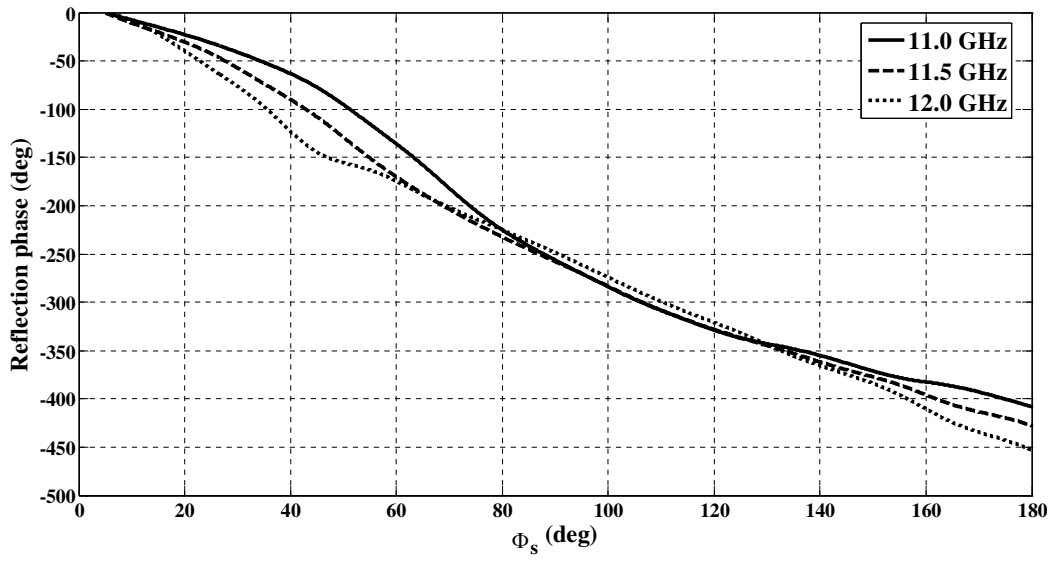


**Figure 3.** Phase of the reflection coefficient for normal incidence at different frequencies.
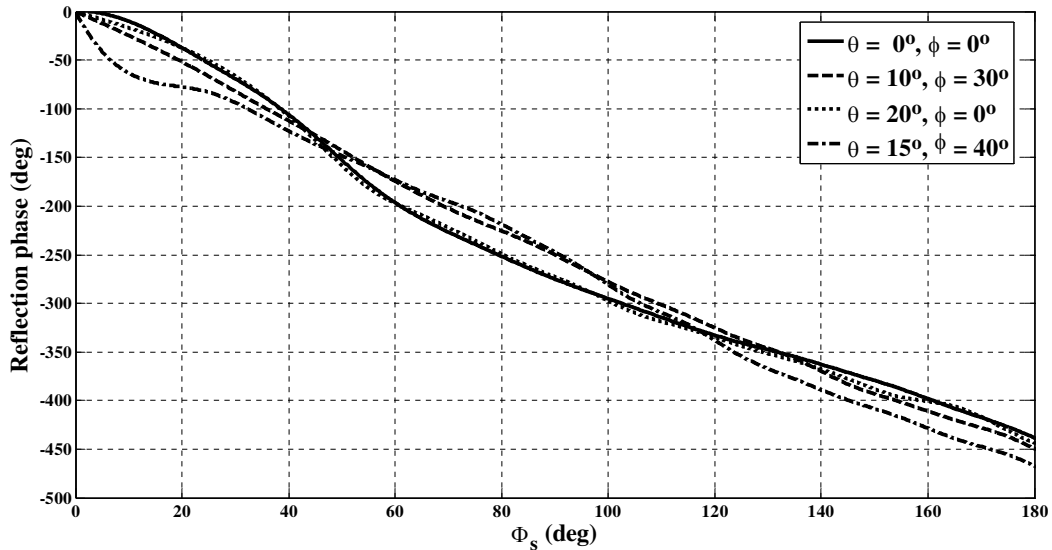


**Figure 4.** Phase of the reflection coefficient for different angles of incidence at 11.5 GHz.
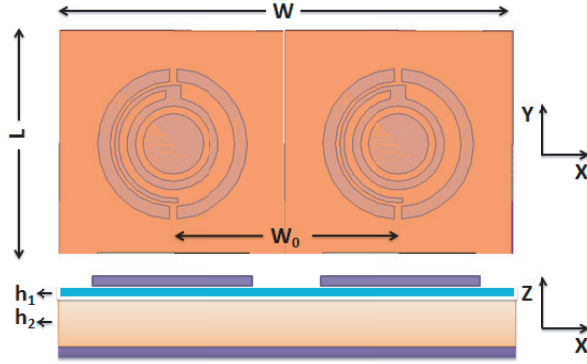
**Figure 5.** Geometry of the designed two-patch element unit cell reflectarray.



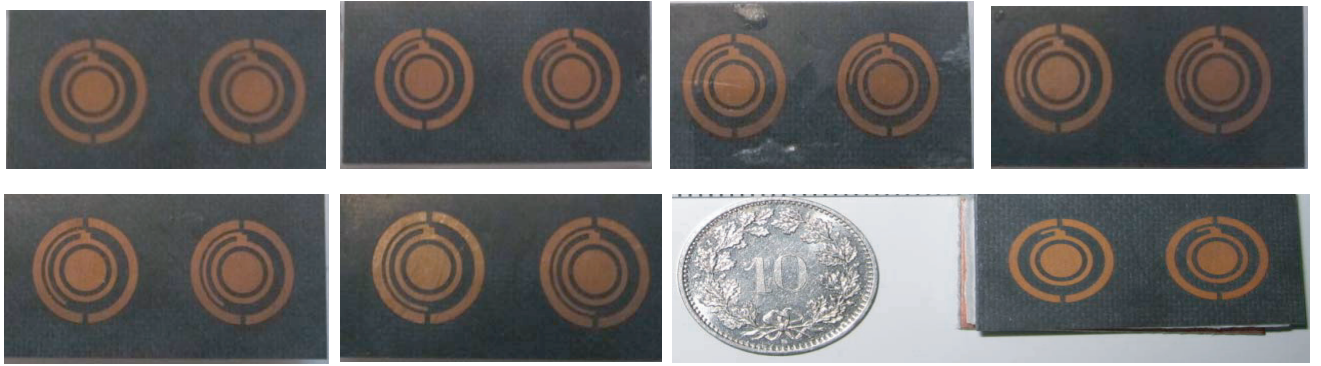**Figure 6.** Measurement setup for scattering element unit cell reflectarray. parameters measurements, Reprint [16].



**Figure 7.** Fabricated samples of reflectarrays at different $\Phi_s = 30°, 60°, 90°, 120°, 150°, 180°$.
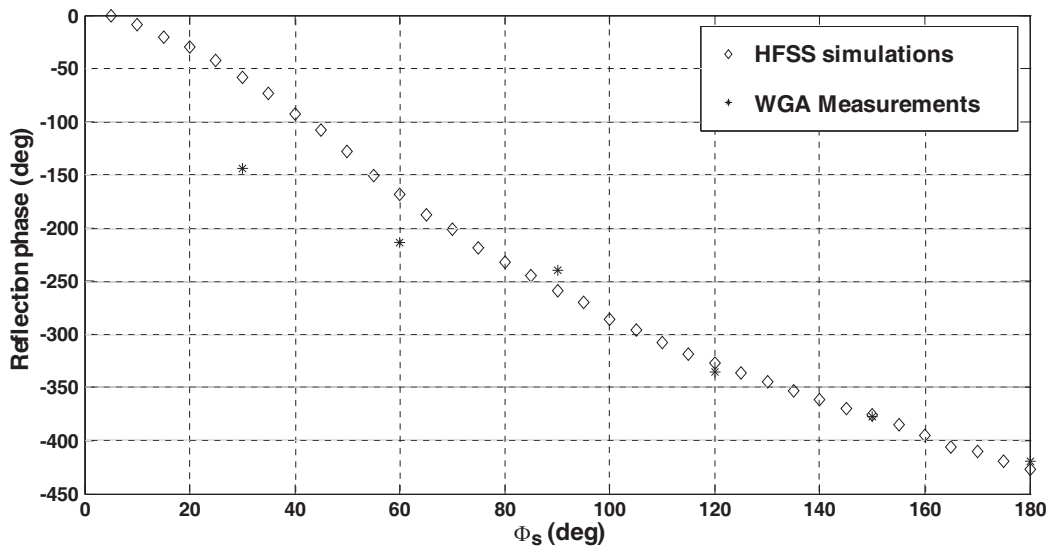


**Figure 8.** Simulated and measured reflection phase versus $\Phi_s$.

Measurements are carried out on six fabricated sets of reflectarray unit cells to obtain six discrete points of reflection phase response. These elements sets have different phases for the corresponding reflected fields, 30°, 60°, 90°, 120°, 150° and 180°.

## 4. MEASURED RESULTS AND DISCUSSION

The measurement procedure in [18] is carried out on fabricated sets of antenna elements as depicted in Fig. 7. The results are compared with the simulated results obtained by Ansoft HFSS software. Fig. 8 shows the simulated and measured reflection phase curves for different $\Phi_s$. The presented results show that the reflection phase response has a sufficient range around 440°. It has a linear variation which shows good overlap with the measured phase samples. At lower values of $\Phi_s$, there is a discrepancy due to the use of C-band tapered waveguide section in measurement setup which controls the incident angle of inbound wave. For smaller values of oblique incidence in Fig. 4, the reflection phase values are affected.

## 5. CONCLUSION

New phasing element for reflectarray is proposed. This element is composed of a phase-delay line attached to a circular ring loaded by a circular disc microstrip patch. It is found to be suitable to achieve 440° linear phase range at central frequency 11.5 GHz. A field perturbation technique using FDTD technique is used to determine the mutual coupling between the nearby elements. Experimental results show the validity of the proposed phasing element in wideband applications.

## ACKNOWLEDGMENT

## REFERENCES

1. Huang, J. and J. A. Encinar, *Reflectarray Antenna*, John Wiley & Sons, Ltd, 2007.
2. Carrasco, E., J. A. Encinar, and M. Barba, "Wideband reflectarray antenna using true-time delay lines," *The Second European Conference on Antennas and Propagation, EuCAP 2007*, 1–6, Edinburgh, 2007.
3. Carrasco, E., J. A. Encinar, and M. Barba, "Bandwidth improvement in large reflectarrays by using true-time delay," *IEEE Transactions on Antennas and Propagation*, Vol. 56, No. 8, 2496–2503, Aug. 2008.
4. Bozzi, M., S. Germani, and L. Perregrini, "Performance comparison of different element shapes used in printed reflectarrays," *IEEE Antennas and Wireless Propagation Letters*, Vol. 2, No. 1, 219–222, 2003.
5. Bialkowski, M. E. and K. H. Sayidmarie, "Investigations into phase characteristics of a single-layer reflectarray employing patch or ring elements of variable size," *IEEE Transactions on Antennas and Propagation*, Vol. 56, No. 11, 3366–3372, Nov. 2008.
6. Ismail, M. Y., M. F. B. M. Shukri, Z. Zakaria, A. F. M. Zain, M. F. L. Abdullah, and M. A. Ubin, "Investigation of static phasing distribution characteristics of passive reflectarray antenna elements," *PIERS Proceedings*, 1218–1222, Moscow, Russia, Aug. 18–21, 2009.
7. Misran, N., R. Cahill, and V. F. Fusco, "Design optimisation of ring elements for broadband reflectarray antennas," *IEE Proceedings — Microwaves, Antennas and Propagation*, Vol. 150, No. 6, 440–444, Dec. 2003.
8. Guo, L., P. K. Tan, and T.-H. Chio, "Bandwidth improvement of reflectarrays using single-layered double concentric circular ring elements," *Progress In Electromagnetics Research C*, Vol. 46, 91–99, 2014.

9. Sayidmarie, K. H. and M. E. Bialkowski, "Phasing of a microstrip reflectarray using multi-dimensional scaling of its elements," *Progress In Electromagnetics Research B*, Vol. 2, 125–136, 2008.

10. Li, Y., M. E. Bialkowski, K. H. Sayidmarie, and N. V. Shuley, "81-element single-layer reflectarray with double-ring phasing elements for wideband applications," *2010 IEEE Antennas and Propagation Society International Symposium*, 1–4, Toronto, ON, 2010.

11. Malfajani, R. S. and Z. Atlasbaf, "Design and implementation of a broadband single-layer reflectarray antenna with large-range linear phase elements," *IEEE Antennas and Wireless Propagation Letters*, Vol. 11, 1442–1445, 2012, doi: 10.1109/LAWP.2012.2228147.

12. Hasani, H., M. Kamyab, and A. Mirkamali, "Broadband reflectarray antenna incorporating disc elements with attached phase-delay lines," *IEEE Antennas and Wireless Propagation Letters*, Vol. 9, 156–158, 2010, doi: 10.1109/LAWP.2010.2044473.

13. Han, C., Y. Zhang, and Q. Yang, "Single-layer reflectarray antennas with improved bandwidth by attaching phase-delay lines," *Proceedings of the 10th European Conference on Antennas and Propagation (EUCAP)*, 1–4, Davos, 2016.

14. Li, Y. and M. E. Bialkowski, "Investigations into electronically controlled rings with arc stubs phasing elements for reconfigurable microstrip reflectarrays," *Asia-Pacific Microwave Conference 2011*, 943–946, Melbourne, VIC, 2011.

15. Li, Y., M. E. Bialkowski, and A. M. Abbosh, "Single layer reflectarray with circular rings and open-circuited stubs for wideband operation," *IEEE Transactions on Antennas and Propagation*, Vol. 60, No. 9, 4183–4189, Sept. 2012, doi: 10.1109/TAP.2012.2207060.

16. Jamaluddin, M. H., R. Gillard, and R. Sauleau, "Perturbation technique to analyze mutual coupling in reflectarrays," *IEEE Antennas and Wireless Propagation Letters*, Vol. 8, No. 1, 697–700, 2009.

17. Ali, W. K. W. and S. H. Al-Charchafchi, "Using equivalent dielectric constant to simplify the analysis of patch microstrip antenna with multi-layer substrates," *IEEE Antennas and Propagation Society International Symposium, 1998*, Vol. 2, 676–679, Atlanta, GA, USA, 1998, doi: 10.1109/APS.1998.702028.

18. Inam, M. and M. Y. Ismail, "Analytical model and practical validation of phase variation of reflect array antenna," *Procedia Engineering*, Vol. 53, 225–232, 2013, ISSN 1877-7058, http://dx.doi.org/10.1016/j.proeng.2013.02.030.